2013

Plasmonics based micro/nano manufacturing

Quincy Jay Garner
Iowa State University

Plasmonics based micro/nano manufacturing

by

Quincy Garner

A thesis submitted to the graduate faculty

in partial fulfillment of the requirements for the degree of

MASTER OF SCIENCE

Major: Mechanical Engineering

Program of Study Committee:

Pal Molian, Major Professor

Abhijit Chandra

Gary Tuttle

Iowa State University

Ames, Iowa

2013

TABLE OF CONTENTS

LIST OF FIGURES

LIST OF TABLES

ACKNOWLEDGEMENT

During my time as a graduate student at Iowa State University, I have received an incredible outpouring of support and advice from numerous people along the way. I thank Dr. Pal Molian for providing academic guidance and his research expertise to my Master's program. He has been the best advisor I could ask for. I want to thank Amy Carver, Dr. Pranav Shrotriya, and the administrative staff of the Mechanical Engineering department for their invaluable support and answers to all of my logistical questions. To the faculty members who have been serving as part of my committee, Dr. Abhijit Chandra and Dr. Gary Tuttle, I greatly appreciate your time and wisdom. To the many fellow graduate students who have helped train and guide me along the way to this point, I am truly appreciative. Finally, I wanted to thank my family and friends for all of their love and support throughout my educational experience. They have been the backbone to my success and the sole reason I have made it this far in life. I am forever grateful for the sacrifices and encouragement they have given me.

ABSTRACT

Since the advent of the Information Age, there has been an ever growing demand to continually shrink and reduce the cost of semiconductor products. To meet this demand, a great amount of research has been done to improve our current micro/nano manufacturing processes and develop the next generation of semiconductor fabrication techniques. High throughput, low cost, smaller features, high repeatability, and the simplification of the manufacturing processes are all targets that researchers continually strive for. To this day, there are no perfect systems capable of simultaneously achieving all of these targets. For this reason, much research time is spent improving and developing new techniques in hopes of developing a system that will incorporate all of these targets. While there are numerous techniques being investigated and developed every year, one of the most promising areas of research that may one day be capable of achieving our desired targets is plasmonics. Plasmonics, or the study of the free electron oscillations in metals, is the driving phenomena in the applications reported in this paper. In chapter 2, the formation of ordered gold nanoparticles on a silicon substrate through the use of energetic surface plasmons is reported. Utilizing a gold/alumina nano-hole antenna and 1064 nm Nd:YAG laser system, semi-periodic gold nanoparticles were deposited onto the surface of a silicon substrate. The novel technique is simpler, faster, and safer than any known gold nanoparticle deposition technique reported in literature. The implementation of this technique has potential wide-ranging applications in photovoltaic cells, medical products, and many others. In chapter 3, a low cost lithography technique utilizing surface plasmons is reported. In this technique, a plasmonic photomask is created by coating a pre-made porous alumina membrane with a thin aluminum layer. A coherent, 337 nm UV laser source is used to expose the photomask and excite surface plasmons along the metal layer. The surface plasmons allow for

features well below the wavelength of the incident light to be produced. Along with this technique, a unique texturing effect was discovered using the same photomask and 400 nm UV lamp source. The developed technique promises to greatly reduce the cost and complexity of sub-100 nm photolithography using only a UV light source and the novel plasmonic photomask.

CHAPTER 1. GENERAL INTRODUCTION

1.1 Motivation

The research problems that are addressed in this thesis can be broken into two main categories. The first problem is the need to develop low cost, simple, and energy efficient techniques for forming and depositing metallic nanoparticles onto the surface of various substrates. Current techniques are limited in these aspects and are thus highly expensive with relatively low throughputs. The second problem that is addressed is the diffraction limit of light in conventional photolithography. Feature sizes produced in conventional photolithography are generally limited to half the wavelength of the exposure source. This limitation introduces additional cost and system complexity when features smaller than 100 nm are fabricated. The research discussed in this thesis is highly significant in that any potential applications could provide a significant paradigm shift to the multi-billion dollar semiconductor industry. With the continuing advancement of consumer electronics at an ever increasing pace, we must continue to improve our fabrication techniques at an equally rapid pace. The work presented in this thesis looks to address this growing demand and provide tangible solutions to some of the issues plaguing current fabrication techniques.

1.2 Thesis Organization

The organization of this thesis is centered upon two journal papers that have been submitted for publication to Nanomaterials and Materials Letters. The contents of these papers explain in depth the methods and results of the research conducted to address the problems listed in the general introduction. Sources specific to each journal entry are located at the end of their

respective chapters. A general conclusions section will follow the second journal article and summarize the findings of each journal entry.

1.3 Review of Literature

I. Current Nanolithography Techniques

While plasmonics may still be in the early stages of development, there has been a great deal of research reporting the underlying physics and potential applications of this phenomenon. One of the most widely reported applications of plasmonics are its potential uses in the lithography process. Lithography has been the mainstream technique for fabricating cutting-edge semiconductor integrated circuits or microelectromechanical systems for the past several decades. There are many lithography techniques used in the semiconductor industry today, and while no technique is perfect, each technique has its own set of advantages and disadvantages. This section of the literature review will discuss some of these nanolithography techniques and compare their advantages and disadvantages.

Electron beam lithography is a method in which a beam of electrons is emitted in a patterned fashion along the surface of a substrate covered with a thin film known as resist [1]. When the electrons come in contact with the resist, the molecules of the resist interact with the electrons, thus changing the solubility of the exposed area. The direction of the electron beam can then be controlled along the substrate and resulting patterns can be formed. Electron beam lithography is advantageous in that its resolution is not limited by the diffraction limit of light, which can allow for linewidths on the order of 10 nm or smaller. Electron beam lithography is however limited by its high system cost and low throughput due to the relatively slow write speeds of the single beam system.

Dip Pen Nanolithography (DPN) uses a technique where an atomic force microscope (AFM) tip is used to pattern images onto a substrate typically using a form of molecular ink coated onto the microscope tip itself [2,3]. DPN is able to produce features under 100 nm depending on the quality of the AFM tip. Similar to electron beam lithography, Dip Pen Nanolithography is limited by the total cost of the system and low throughput.

Electron beam lithography and Dip Pen Nanolithography are two types of systems that fall into the category of maskless lithography. Maskless lithography is a type of printing that involves the direct writing of patterns onto substrates. Lithography using a mask on the other hand is a common nanoscale printing technique where a "stensil" or mask is made with pre-defined patterns that can be reused to print the same pattern multiple times on different substrates. The advantage of using a mask is that it typically allows for a much higher throughput than maskless techniques, but can be disadvantageous in that it is less versatile than maskless techniques. Electron beam lithography and Dip Pen Nanolithography are commonly used in the production of masks for other nanolithography techniques.

In Nanoimprint Lithography (NIL), a 3-D stamp mask is made with a pre-formed pattern that is desired to be shaped onto a substrate[4-6]. The mask is then stamped onto a material coated with a polymer resist and heat and pressure is applied. The mask is then lifted from the surface and the residual resist is etched away, leaving behind the fully patterned resist. The NIL technique addresses the problems of low throughput and high cost, but new issues of limited repeatability and contamination arise. The masks used in NIL are often very fragile and can be easily damaged when removed from the substrate, which greatly limits the lifetime of the masks and repeatability of the process.

By far the most common lithography technique in use today is photolithography. Photolithography is a process that uses light to transfer a pattern from a mask onto a substrate coated with a light sensitive resist. When light of a certain frequency interacts with the molecules of the resist, the solubility of the exposed area changes, allowing specific sections of the substrate to be patterned. Similar to Nanoimprint Lithography, the resist is chemically treated to engrave the exposure pattern into the substrate and enable the deposition of a new material in the desired pattern where the photoresist once was. Photolithography is praised for its high throughput, as most resists can be exposed within a few seconds. The high durability and reusability of the optical masks used in photolithography is also highly regarded. The main concern with photolithography is its potential low resolution due to the diffraction limit of light. In general, the smallest feature sizes that can be printed during photolithography is of the same order as half the wavelength of the incident exposure light. To increase this resolution, the wavelength of the incident light can be shortened or the numerical aperture can be increased. The shortening of the incident wavelength is the main idea behind X-ray and extreme UV photolithography [7,8]. Just as their names imply, these techniques make use of x-ray and extreme UV wavelength light sources impinged on the mask to pattern the photoresist on the substrate. These shorter wavelengths allow for features as small as 20 nm to be formed while maintaining the high throughput and mask durability of longer wavelength techniques. The main concern with these short wavelength lithography techniques is that the cost of each of these systems begins to skyrocket as the incident wavelength begins to shrink. These systems can also be quite complex and difficult to operate safely. Other techniques based on increasing the numerical aperture of the mask have been developed, but are limited by low light transmission due to diffraction and scattering. As the amount of light that reaches the photoresist decreases, the

exposure time begins to increase, and the feasibility of the system comes into question due to long production times.

II. Plasmonic Nanolithography

In an attempt to capture all of the positive aspects of photolithography and form a superior nanolithography system, plasmonic nanolithography was developed. Plasmonic nanolithography is based upon the theory of surface plasmon polaritons (SPPs). Surface plasmons are collective localized electrons existing on the interface of a metal and dielectric material. Surface plasmons have a unique dispersion relation and thus potentially a unique wavelength from the incident light that induced the SPPs. The dispersion relation for SPPs is given as:

$$k_{sp} = \left(\frac{2\pi}{\lambda_0}\right)\sqrt{\frac{\varepsilon_d \varepsilon_m}{\varepsilon_d + \varepsilon_m}} = \frac{2\pi}{\lambda_{sp}}$$

where λ_0 is the incident light wavelength in vacuum, ε_d is the permittivity of the dielectric material, and ε_m is the permittivity of the metal material. By properly selecting the permittivities of the materials used, the wavelengths of the SPPs can be significantly lower than that of the incident light. Using this phenomena, a nanolithography system can be developed that effectively overcomes the diffraction limit of the incident light while maintaining the lower cost and simplicity of a system with longer wavelength incident light.

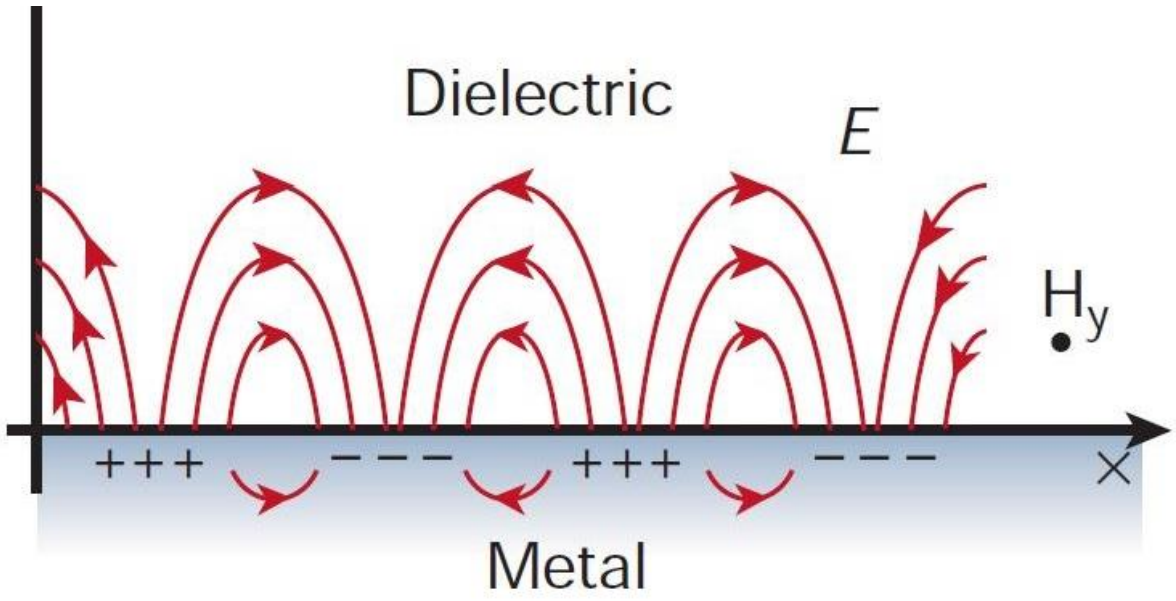

Figure 1. SPPs along metal/dielectric interface (nature.com)

Surface plasmons exist in two basic forms, localized and propagating. Along the metal-dielectric interface, the SPPs wave propagates as an evanescent electromagnetic wave resulting from the collective oscillations of the free electrons in the conduction band on the metal surface. In most cases, SPPs are not easily excited due to the momentum difference between the incident light waves and the waves of the surface plasmon. To compensate for this, periodic hole or nanosphere arrays that are properly tuned can account for the momentum mismatch and excite the SPPs [9,10].

Localized surface plasmons (LSPs) do not propagate in the horizontal plane, but rather as localized electromagnetic fields near the surface of isolated nanoparticles. The transmission of light in a single subwavelength aperture can be enhanced due to the existence of LSPs. For periodic subwavelength apertures, the total transmission enhancement is explained as the integrated effect of LSPs and SPPs. This periodic enhancement is explained by the following equation:

$$\lambda_{\max}(i,j) = P(i^2 + j^2)^{-\frac{1}{2}} \sqrt{\frac{\varepsilon_1 \varepsilon_2}{\varepsilon_1 + \varepsilon_2}},$$

where $\lambda_{\max}(i,j)$ is the wavelength of peak light transmission, P is the lattice constant, i and j are the scattering orders from the array, ε_1 and ε_2 are respectively the dielectric constant of the metal and the dielectric materials. Each peak of the light transmission is labeled by a set of integers (i, j). Numerical simulations have shown that resolutions as high as 20 nm can theoretically be achieved using illumination light of 365 nm by taking advantage of surface plasmon resonance and periodic array subwavelength apertures.

III. Plasmonic Lens

By taking advantage of the SPP effect and periodic subwavelength apertures, several plasmonic lenses have been developed using various techniques. These techniques are generally separated into three main categories: contact nanolithography, planar lens imaging nanolithography, and direct writing nanolithography. In the contact method, the photoresist is exposed by SPPs originating from the metal mask. Since SPPs can only travel tens of nanometers, intimate contact between the mask and photoresist is required. The planar lens imaging method uses a superlens placed underneath the mask to project nanopatterns through the mask and onto the photoresist. This sub-diffraction imaging is made possible by materials with a negative index of refraction bending light into a negative angle with respect to the surface normal. Finally, the direct writing method as discussed before, is a plasmonic nanolithography system that does not invoke the use of a mask to form nanopatterns on a substrate.

Now that the three basic types of plasmonic nanolithography systems have been established, some of the specific lenses that have been proposed and developed can be discussed.

Liu, Srituravanich, et al. created two very basic plasmonic lenses using structures milled into a thin metal film and placed on a quartz substrate [11]. In the first technique, circles of varying diameter were cut through a 150 nm thick silver film. The average slit width for these circles being 283 +/- 23 nm. In the second technique, elliptical shapes with a semi-major axis length of 4 μm and semi-minor axis length of 2.5 μm were milled into 70 nm thick aluminum films. In both techniques, the metal films were then deposited onto a quartz substrate and 514 nm incident wavelength light was used. The transmission of SPPs through these lenses was observed and then modeled using Microwave Studio.

Srituravanich, Pan, et al. created a "flying plasmonic lens" intended to be a low cost, high throughput, maskless nanolithography system [12]. While keeping the design of the plasmonic lens similar to the one mentioned earlier, the true innovation in this technique is the system used to create a nanoscale air gap between the plasmonic lens and the substrate during the high-speed writing process. The developed technique involves a novel air-bearing slider to "fly" the plasmonic lens arrays at a height of 20 nm above the substrate at speeds between 4 and 12 $^{m}/_{s}$. The rotation of the substrate creates an air flow beneath the surface of the plasmonic flying head, known as the air bearing surface. The air bearing surface generates an aerodynamic lift force and is balanced with the force supplied by a suspension arm to precisely regulate the gap between the plasmonic lens array and the rotating substrate.

While many plasmonic lenses are based around the concept of periodic subwavelength nanohole arrays, recent research has shown that sharp ridged apertures in metal may provide equal transmittance and possibly even greater spatial resolution compared to their counterpart. Grober, et al. first proposed the bowtie aperture to be used in sub-diffraction optics as an optical probe at microwave frequencies [13]. Xu, et al. were the first to use the bowtie antenna in a

plasmonic lens [14]. Bowtie apertures with a 30 nm gap size were fabricated in 150 nm thick aluminum film and deposited on a quartz substrate. Using this technique, sub-50 nm linewidths were achieved.

More recently, plasmonic lenses tailored for more traditional 365 nm UV incident light have been developed [15, 16]. The design of these lenses is based around an aluminum layer perforated with 2D periodic hole arrays surrounded by a dielectric layer of quartz on top and dielectric PMMA below. A negative photoresist layer (SU-8) was then spun coated onto the PMMA layer to eliminate any air gap between the mask and the photoresist. Using this lens, sub-100 nm dot arrays were patterned with exposure times under 10 s.

Yang, Zeng, et al. developed a plasmonic lens designed for 193 nm (Deep UV) wavelength by using multiple metal-dielectric interfaces [17]. For this plasmonic lens, 8 pairs of GaN/Al multi-layers are stacked together onto a PMMA substrate. The incident light is sent through the PMMA layer as well as an optical mask shaped in the desired pattern. The light reaches the multi-layers and surface plasmons are induced at each of the metal-dielectric interfaces. Using this lens, features as small as 22 nm were observed.

While these are just a few examples of the plasmonic lenses that have recently been developed, there are plenty of others not discussed that have been proposed just in the past few years alone[18-22]. Although it may seem that with the development of so many unique plasmonic lenses that little work is left to be done in this field, the opposite is actually true. Some of the challenges that need to be addressed in the design of future plasmonic lenses are low light transmission resulting in long production times, high cost of lens fabrication, and the lack of a large exposure area in a massively parallel scheme. While many issues still remain, plasmonic

nanolithography remains a promising technique for the next generation of nanolithography with its vast potential for high throughput, excellent resolution, and cost effectiveness.

IV. Formation of Gold Nanoparticles

There are several established techniques that are in widespread use that are capable of forming gold nanoparticles. These fabrication techniques can be split into the two main categories of chemical synthesis and thermal ablation. Chemical synthesis, or the purposeful execution of a chemical reaction to obtain a final product, can be used to isolate gold from other chemical products. These chemical reactions can often be controlled to produce gold nanoparticles of varying size and shape. Thermal ablation, or the selective heating of a specific target area, can be used to create metallic nanoparticles by introducing a selective heating system (usually a focused laser) to a metal source. The heating system will form and remove metallic nanoparticles from the source metal during the ablation process. The size and shape of the metallic nanoparticles can be manipulated by adjusting the area of thermal exposure and by the type of heating source used. Specific examples of developed techniques for creating gold nanoparticles will be discussed further in chapter 2.

The utilization of surface plasmon resonance in the aided formation of gold nanoparticles is a relatively new reported process. Through the introduction of laser light impinged on metal film at surface plasmon resonance conditions, thermal ablation of metallic film can occur at lower threshold fluence values than previously reported. The use of air/Au film/glass under the second harmonic of a Q-switched Nd:YAG laser (532 nm) with pulse power density slightly lower than the ablation threshold limit of gold film has been shown to result in the nanostructuring of gold particles [23]. This reported effect paves the way for future fabrication

processes utilizing surface plasmon resonance in the formation of gold nanoparticles and is a basis for some of the results detailed in chapter 2.

1.4 Proposed Projects

In the projects discussed in this thesis, we looked to address many of the issues discussed in the literature review. In the first project, we examined the potential applications of plasmonics in gold nanoparticle formation. In the second project, we looked to overcome some of the issues plaguing UV plasmonic nanolithography by developing a nanolithography system based on a newly proposed plasmonic lens. The main issues we wanted to address include the simplicity of the system, fabrication cost, and total energy fluence of the fabrication process. The specific tasks that we hoped to achieve in these projects included:

1. Fabricate a plasmonic lens using nanoporous alumina membrane (PAM) coated with a thin metal layer tailored to the desired parameters of the plasmonic lens, i.e. hole shape, diameter, periodicity.
2. Generate SPPs through UV laser beam interaction with the plasmonic lens developed in (1), and understand the transfer of SPP into high-intensity light with spatial patterns through coherent interference of multiple scattered SPP waves in the near field.
3. Perfom nanolithography by producing subwavelength features as small as 20 nm and characterizing the feature size, accuracy, repeatability, and collateral thermal damages using scanning electron microscopy (SEM) and atomic force microscopy (AFM).
4. Develop a plasmonic optical nano-antenna capable of producing metallic nanoparticles at lower laser energy fluence than any previously reported study.

The novel features of our proposed nanolithography system are the use of a low cost UV laser for the excitation of SPPs, and a new, inexpensive, and easy to fabricate plasmonic lens based on nanoporous alumina. The novel features of the plasmonic nano-antenna system include the use of periodic alumina structures to create semi-periodic metallic structures and the use of plasmonics in a nanostructuring system to lower the total energy fluence.

When designing the alumina pore features and metal film used in the plasmonic mask to excite SPPs along the PAM interface, great care must be taken in determining these parameters. Gold, silver, and aluminum have all been shown to excite surface plasmons due to their negative dielectric constants under certain wavelengths, and are thus good candidates for use in a plasmonic lens. In order for surface plasmons to be excited, the real part of the dielectric constant of the metal film must be negative and its magnitude must be larger than that of the surrounding dielectric material (PAM). To calculate the dielectric constant, or relative permittivity of a material, the following equation is used,

$$n = \sqrt{\varepsilon_r \mu_r}$$

where n is the refractive index of a material, ε_r is the material's relative permittivity, and μ_r is the material's relative permeability. Knowing the wavelength of the light that is incident on the material, we can determine the refractive index of that material, and thus determine the material's relative permittivity [24,25].

For the plasmonic lens setup, we will be using UV light sources between 337-405 nm. Using this information, it was determined that the relative permittivities of gold, silver, and aluminum will approximately be $-0.26 + 6.66i$, $-1.01 + 0.58i$, and $-16.3 + 2.74i$ at 337 nm. The relative permittivity of alumina under UV wavelengths was determined to be 3.24. It must

also be noted that the Drude model for determining the dielectric constant of metals can also be used to confirm these results. It was determined that aluminum would be the best option to excite SPPs under UV wavelengths since the magnitude of the real part of the dielectric constant is greater than that of the PAM. This idea is supported with literature for UV excitation of SPPs [26]. SU-8 and AZ-5214E will be used as the negative and positive photoresists due to their high absorption in the UV and deep UV range.

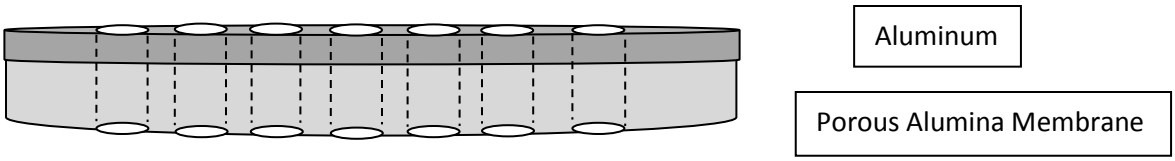

Figure 2. Side view of proposed plasmonic lens (porous alumina membrane with thin aluminum coating)

In the plasmonic nano-hole antenna setup, we will be using a 1064 nm Nd:YAG laser source. This higher energy source will be able to provide short, powerful pulses capable of thermal ablation of various metals under infrared wavelengths. In this setup, gold was determined to be the best option to excite SPPs due to its high plasmonic response under infrared wavelengths compared to other metals. A silicon wafer will be used as the base substrate for depositing the gold nanoparticles as it is the industry standard for semiconductor substrates. The experimental methods and results of these two projects will be discussed in detail in the next two chapters.

References

1. Dhaliwal, R. S.; Enichen, W. A.; Golldaday, S. D.; Gordon, M. S.; Kendall, R. A.; Lieberman, J. E.; Pfeiffer, H. C.; Pinckney, D. J.; Robinson, C. F.; Rockrohr, J. D.; Stickel, W.; Tressler, E. V. (2001). *IBM J. Res. Dev*. ***45***. 615−638.

2. Piner, R. D.; Zhu, J.; Xu, F.; Hong, S.; Mirkin, C. A. (1999). *Science*. ***283***. 661−663.

3. Zhang, H.; Chung, S.-W.; Mirkin, C. A. (2003) *Nano Letters.* ***3.*** 43−45.

4. Chou, S.Y.; Krauss, P.R.; Renstrom, P.J. (1996). "Imprint Lithography with 25-Nanometer Resolution". *Science* **272.** (5258): 85–7.

5. Colburn, M.; Bailey, T.; Choi, B. J.; Ekerdt, J. G.; Sreenivasan, S. V.; Willson, C. G. (2001). *Solid State Technology***.** ***44***. 67−78.

6. McAlpine, M. C.; Friedman, R. S.; Lieber, C. M. (2003). *Nano Letters*. ***3***. 443−445.

7. Lin BJ. (1975). "Deep UV Lithography". *Journal of Vacuum Science and Technology*. ***12***. 6, 1317-1320.

8. Early, K; Schattenburg, M; Smith, H (1990). "Absence of resolution degradation in X-ray lithography for λ from 4.5nm to 0.83nm". *Microelectronic Engineering*. **11**. 317.

9. Zhang YK, Dong XC, Du JL, Wei XZ, Shi LF, Deng QL, Du CL (2010) "Nanolithography method by using localized surface plasmon mask generated with polydimethylsiloxane soft mold on thin metal film". Opt Lett **35**. 13, 2143–2145.

10. Degiron A, Ebbesen TW. "The role of localized surface plasmon modes in the enhanced transmission of periodic subwavelength apertures." *Journal of Optics A-Pure and Applied Optics*. **7**, 2, S90-S96.

11. Liu ZW; Steele JM; Srituravanich W; et al. (2005). "Focusing Surface Plasmons with a Plasmonic Lens." *Nano Letters*. **5.** 9, 1726-1729.

12. Srituravanich Werayut; Pan Liang; Wang Yuan; et al. (2008). "Flying Plasmonic Lens in the near field for high speed nanolithography." *Nature Nanotechnology*. **3.** 12, 733-737.

13. Grober RD, Schoelkopf RJ, Prober DE (1997) Optical antenna:towards a unity efficiency near-field optical probe. Appl Phys Lett 70(11):1354–1356.

14. Wang L, Uppuluri SM, Jin EX, Xu XF (2006) Nanolithography using high transmission nanoscale bowtie apertures. Nano Lett 6 (3):361–364.

15. Srituravanich W, Durant S, Lee H, Sun C, Zhang X (2005) Deep subwavelength nanolithography using localized surface plasmon modes on planar silver mask. J Vac Sci Technol B 23(6):2636–2639.

16. Srituravanich W; Fang N; Sun C; et al. (2004) "Plasmonic Nanolithography." *Nano Letters.* **4**. 6, 1085-1088.

17. Yang Xuefeng; Zeng Beibei; Wang Changtao; et al. (2009). "Breaking the feature sizes down to sub-22 nm by plasmonic interference lithography using dielectric-metal multilayer." *Optics Express.* **17**. 24, 21560-21565.

18. Liu Yuxiang; Xu Hua; Stief Felix; et al. (2011). "Far-field superfocusing with an optical fiber based surface plasmonic lens made of nanoscale concentric annular slits." *Optics Express*. **19**. 21, 18072-18079.

19. Miao Junjie; Wang Yongsheng; Guo Chuanfei; et al. (2011). "Plasmonic Lens with Multiple-Turn Spiral Nano-Structures." *Plasmonics*. **6**. 2, 227-233.

20. Zentgraf Thomas; Liu Yongmin; Mikkelsen Maiken H.; et al. (2011). "Plasmonic Luneburg and Eaton Lenses." *Nature Nanotechnology*. **6**. 3, 151-155.

21. Wang Jun; Zhou Wei. (2010). "Experimental Investigation of Focusing of Gold Planar Plasmonic Lenses." *Plasmonics*. **5**. 4, 325-329.

22. Hao Fenghuan; Wang Rui; Wang Jia. (2010). "A Design Method for a Micron-Focusing Plasmonic Lens based on Phase Modulation." *Plasmonics*. **5**. 4, 405-409.

23. Fedorenko L; Mamykin S; Lytvyn O. (2011). "Nanostructuring of Continuous Gold Film by Laser Radiation Under Surface Plasmon Polariton Conditions." *Plasmonics*. **6**. 2, 363-371.

24. *Aleksandar D. Rakić. Algorithm for the determination of intrinsic optical constants of metal films: application to aluminum, Appl. Opt. 34, 4755-4767 (1995).*

25. *Sopra N&K Database*

26. Sreekanth K. V.; Murukeshan V. M. (2010). "Effect of metals on UV-excited plasmonic lithography for sub-50 nm periodic feature fabrication." *Applied Physics A-Materials Science and Processing.* **101**. 1, 117-120.

CHAPTER 2. FORMATION OF GOLD NANOPARTICLES BY ABLATION WITH SURFACE PLASMONS

A paper to be submitted to Nanomaterials

*Quincy Garner and Pal Molian

*corresponding author

The formation of ordered gold nanoparticles on a silicon substrate through the use of energetic surface plasmons is reported. A laser-assisted plasmonics system was assembled and tested to synthesize gold nanoparticles from gold thin film by electrical field enhancement mechanism. A mask containing an array of 200 nm diameter holes with a periodicity of 400 nm was prepared and placed on a silicon substrate. The mask was composed of 60 μm thick porous alumina membrane sputter-coated with 100 nm thin gold film. A Nd:YAG laser with 1064 nm wavelength and 230 μs pulse width (free-running mode) was then passed through the mask at an energy fluence of 0.35 J/cm^2. The extraordinary transmission of laser light through alumina/gold nano-hole optical antenna created both extended and localized surface plasmons that caused the gold film at the bottom of the mask to fragment into nanoparticles and deposit on the silicon substrate that is in direct contact with the mask. The surface plasmon method is simpler, quicker, energy efficient, contamination-free, and environmentally safer than existing physical and chemical methods and can be extended to all types of materials that will in turn allow for new possibilities in the formation of nanostructured surfaces, the creation of plasmonic devices, and other wide ranging applications.

Keywords: Laser – plasmons – gold – nanoparticles – porous alumina membrane

I. Introduction

Plasmonics is a rapidly emerging technology for photonics, sensors, microscopy, data storage, and lithography. However, there is little work reported on the use of plasmonics for nanoscale manufacturing applications such as nanomachining and nanoparticle synthesis [1-3]. The coherent interference of surface plasmon polaritons was able to produce 50-70 nm diameter holes in silicon wafers [1]. Plasmonic effects strongly affected the aspect ratio of nanometer-sized holes in femtosecond laser ablation if the surface plasmon resonance conditions were met [2]. Nanofragmentation of gold thin films by 532 nm, 10 ns laser radiation in the system air/gold film/glass was achieved at surface plasmon resonance conditions [3]. The plasmonic effects aided in reducing the energy fluence required for thermal ablation and permitted self-organization of micro-ablation events [3].

Gold nanoparticles play a vital role in biology, chemistry, optics and microelectronics by virtues of a large surface-to-volume ratio, quantum confinement, and other unique properties. For example, gold nanoparticles are extensively used in life sciences for labeling, delivery, heating, and sensing due to their strong absorption, scattering, plasmon resonance, x-ray contrasting and functionalization with ligands. The development of highly ordered, uniform gold nanoparticles is also useful to the advancement of plasmonic devices. Gold nanoparticles could act as a surface coupler and, under certain size and periodicity conditions, can help in the transmission of sub-diffraction limited light. New applications of gold nanoparticles are constantly emerging in many areas such as fuel cells, cancer cell therapy, nanoimprinting and solar cells [4-6].

Many physical and chemical techniques are available to generate gold nanoparticles [7-20]. Pulsed laser ablation (PLA) in gas and liquid media appear to lead among all physical processes. When the energy fluence of a laser beam exceeds that of the ablation threshold of gold, fragmentation occurs in the form of ions, electrons and neutrals at the irradiated spot forming nanoparticles. Despite the availability of a number of physical and chemical processes for gold nanoparticles, there are still many issues that need to be addressed in the form of particle size and uniformity, production rate, simplicity, contamination, energy efficiency and system cost. In this paper, we present a method capable of producing gold nanoparticles through the excitation of surface plasmons that addresses many of these problems.

II. Theory

Plasmonics has been known by scientists for many decades, yet its applications to photonics, microelectronics and medicine have just begun to be realized within the past decade [21]. Surface plasmons (SP) are the collective and coherent oscillations of conduction electrons in a metal film present at the interface of metal-dielectric with permittivities of opposite sign. Energy can be harnessed when the electrons are coupled with photons by creating quasiparticles called polaritons. SPs are easier to produce in metals that exhibit a dielectric function with large negative real number and small imaginary number. Common metals that fulfill this requirement under certain wavelengths are silver, gold and aluminum.

SPs propagate along the interface between a metal and dielectric, which is typically perpendicular to the incident light. Figure 1 shows a coordinate system where $z > 0$ is the dielectric, $z < 0$ is the metal, and the metal-dielectric interface is in the x-y plane.

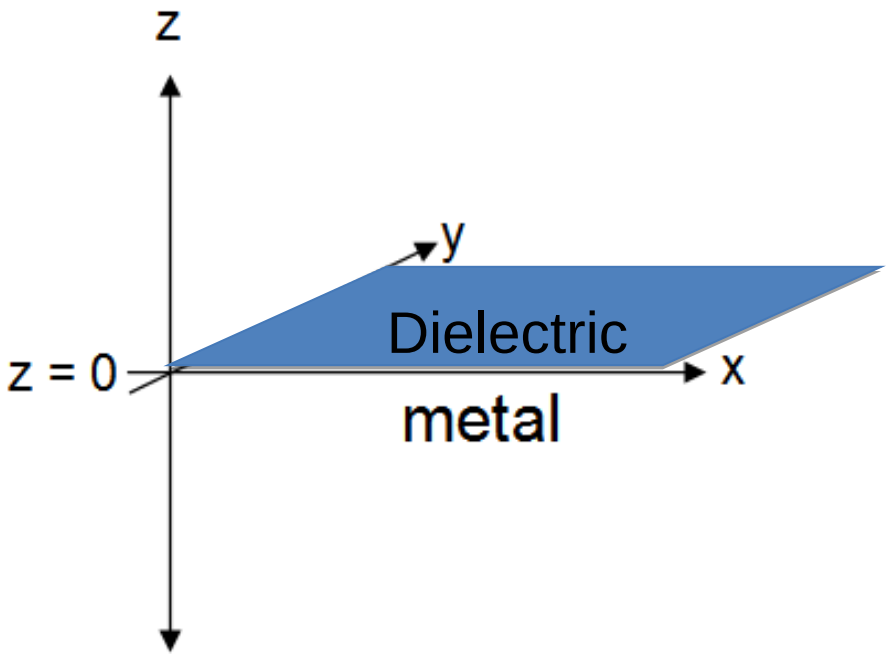

FIG. 1. The coordinate system used for the description of surface plasmons

It may be noted that SPs are purely longitudinal surface charge density waves unlike other electromagnetic waves. The plasmon wavevector, k_x, is related to the angular frequency, ω, of the incident light through the dispersion relationship [22]:

$$k_x = k_{sp} = \left(\frac{2\pi}{\lambda_0}\right)\sqrt{\frac{\varepsilon_d \varepsilon_m}{\varepsilon_d + \varepsilon_m}} \quad (1)$$

Where $k_x = k_{sp} = 2\pi/\lambda_{sp}$ with λ_{sp} the plasmon wavelength, λ_o the incident laser wavelength, ε_m (λ_o) and ε_d (λ_o) are the dielectric functions of the metal and dielectric material respectively. An important attribute of SPs is their potential for a shorter wavelength and higher intensity compared to the incident light. It should be noted that the dielectric function of metal is a complex wavevector with $\varepsilon_m = \varepsilon_m' + i\varepsilon_m''$ while for the dielectric it is a real number. The amplitude of SPs decreases with increasing propagation distance in the x-direction and eventually dissipates. The propagation distance L along the metal surface is given by:

$$L = \frac{1}{k_0}\left(\frac{\varepsilon_d + \varepsilon_m'}{\varepsilon_d}\right)^{3/2} \frac{(\varepsilon_m')^{1/2}}{\varepsilon_m''} \quad (2)$$

The wavevector perpendicular to the interface, k_z, corresponds to electric fields that decay exponentially with increasing distance from the interface. The penetration depth is defined as the distance from the interface of metal-dielectric at which the amplitude is reduced to 35% of the initial value. The penetration depths and permittivites are related by:

$$-z_m/\varepsilon_m' = z_d/\varepsilon_d \quad (3)$$

where z_m and z_d are the penetrations in metal and dielectric respectively. The penetration depth in metal is usually smaller than in dielectric due to considerable energy losses.

The extraordinary optical transmission phenomenon, originally discovered in nano-hole arrays of metal thin films, is attributed to the excitation of SPs that exist in two basic forms: localized (LSP) and extended (ESP) [23]. LSPs are localized electromagnetic fields near the surface of isolated nanostructures while ESPs propagate in the horizontal plane. LSP depends on the shape and size of the hole while the ESP is a function of the periodicity. Both SPs contribute to the enhanced transmission. In most cases, SPs are not easily excited due to the momentum difference between the incident light waves and the waves of SPs. To compensate for this, periodic arrays in thin films can be properly tuned to account for the momentum mismatch and consequent excitation of SPs [24, 25].

The transmission of light in a single sub-wavelength aperture can be enhanced due to the existence of LSPs. For periodic sub-wavelength apertures, the total transmission is based on the integrated effect of LSP and ESP. The maximum transmission depends on the period of the nano-hole array, the incidence angle and the polarization of the excitation light. The transmission

of light in nano-hole arrays is much higher than expected from classic diffraction theory implying that even the light impinging on the metal between the holes can also be transmitted. In other words, the whole periodic structure acts like an antenna in the optical regime. The transmission spectra of hole array display peaks that can be tuned by adjusting the period and the symmetry is given by the following equation:

$$\lambda_{\max}(i,j) = P(i^2 + j^2)^{-\frac{1}{2}} \sqrt{\frac{\varepsilon_m \varepsilon_d}{\varepsilon_m + \varepsilon_d}} \quad (4)$$

where $\lambda_{\max}(i,j)$ is the wavelength of peak light transmission, P is the periodicity, i and j are the scattering orders from the array, ε_m and ε_d are respectively the dielectric constant of the metal and the dielectric material. Each peak of the light transmission is labeled by a set of integers (i, j).

The oscillatory nature of the surface modes enables the resonant enhancement of the highly confined electromagnetic fields. At the resonance, the intensity of the electric field at the interface between the metal and the dielectric is strongly enhanced due mainly to the smaller complex permittivity of the dielectric compared to the metal. SPs can enhance the electrical field by as high of a factor as 1000. Nanofocusing, or the strong localization of the optical energy in regions smaller than possible by the diffraction limit, can offer promising applications in nanofabrication. In summary, when the incident light illuminates the nano-hole array, localized and extended SPs are excited under surface plasmon resonance conditions. The nano-hole array with SPs as electrical dipoles acts as an optical antenna with the potential capability for nanoscale material removal.

III. Experiment

Figure 2 illustrates the underlying physical mechanism involved in the experiment and its projected effect on the formation of metallic nanoparticles. In this setup, there are three main components: metal/dielectric mask, silicon substrate and 1064 nm laser.

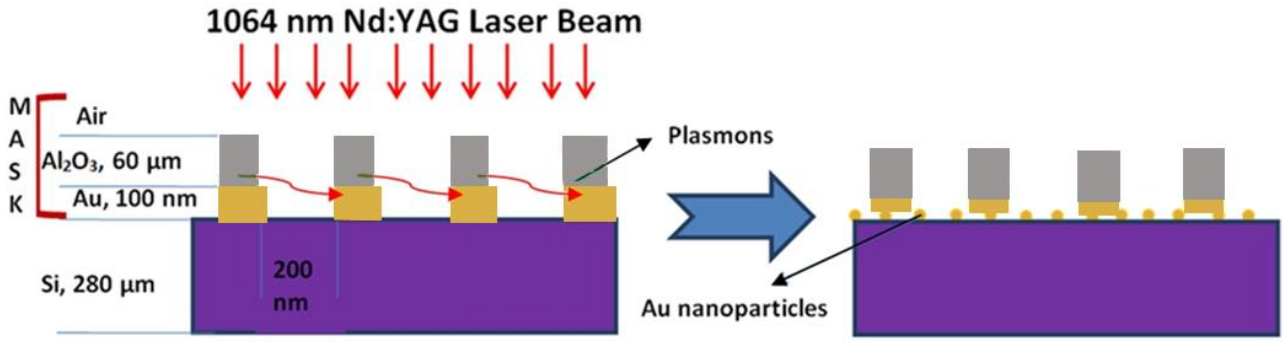

FIG. 2. Schematic diagram of experimental excitation of surface plasmons and the resulting formation of nanoparticles

The mask is prepared as follows: porous alumina membranes with a diameter of 25 mm (Anodisc25™) were received from Whatman. Anodisc25 is composed of a high purity alumina matrix manufactured by electrochemical methods. It has a precise, non-deformable honeycomb pore structure with no lateral crossovers between individual pores. The membrane has an average thickness of 60 µm, pore diameter of 200 nm and periodicity of 400 nm. Figure 3 shows the scanning electron micrograph image of the membrane. Sputtering was then employed using a Denton Vacuum Desk V at 40 mTorr of pressure for 200 seconds to deposit a 100 nm thin film of gold on the bottom side of the membrane. The dielectric alumina nano-hole array pattern and thin metal gold film combination serves as an optical antenna for light transmission.

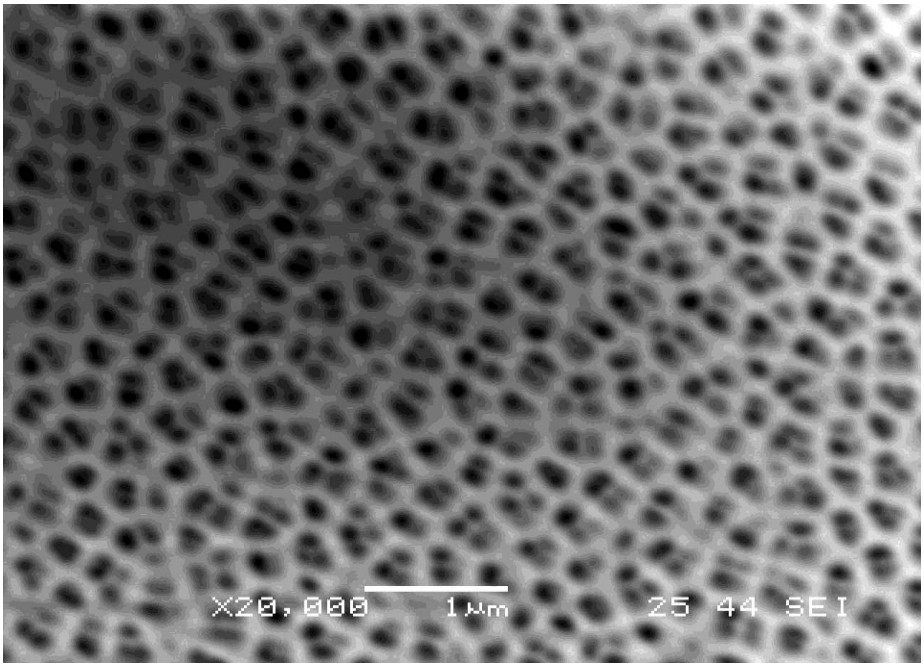

FIG. 3. SEM image of porous alumina membrane

Silicon wafers (p-type Si:B (100)) were acquired from University Wafers (66 N Street Unit #9 South Boston, MA 02127). The wafers had a diameter of 25 mm and thickness of 280±25μm. One side of the wafer was polished while the other side was etched using an alkaline solution.

The laser system used was a Q-switched Nd:YAG laser (Spectra Physics, INDI series) along with beam delivery system and positioning table as shown in Fig.4. The laser can be operated in Q-switched mode with a pulse width of 10 ns or in free-running mode with a pulse width of 230 μs. The maximum average power of the laser is 3 W with a maximum possible repetition rate of 10 Hz.

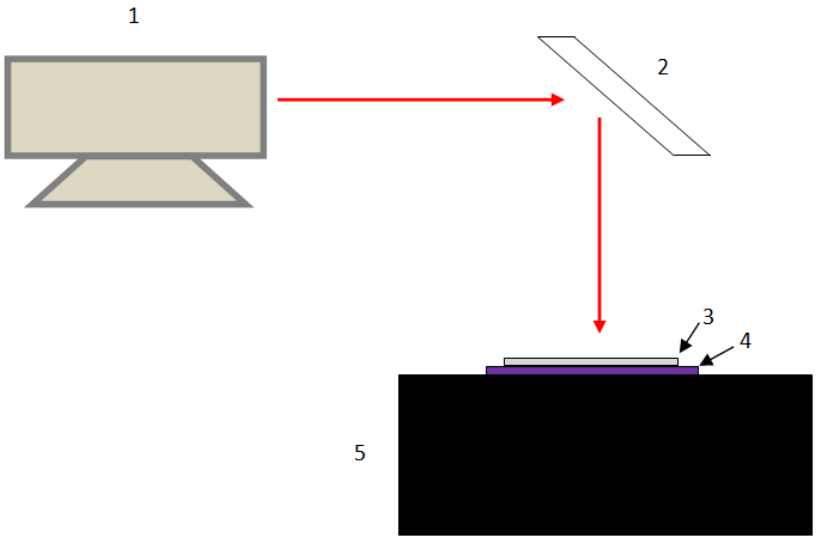

FIG. 4. Basic experimental setup: 1. Nd:YAG laser; 2. beam delivery system; 3. mask; 4. silicon substrate; 5. positioning stage

The experiments consisted of placing the gold-sputtered membrane in direct contact with the polished side of the silicon wafer in an ambient, low humidity environment followed by the passage of the Nd:YAG laser beam through the mask. The 6 mm diameter, p-polarized beam emitted from the laser resonator was delivered to the mask through a 90 degree steering optics without focusing by a lens. The pulse repetition rate was held constant at 1 Hz. Only a single pulse was used for each experiment. The average power of the laser was varied from 0.1 W to 0.5 W. Two pulse widths, 10 ns and 230 μs, were investigated. In addition, experiments were conducted with masks having either only top side gold thin film or without any gold film. Optical microscopy, scanning electron microscopy, and atomic force microscopy were then used to examine the particle size and distribution of gold nanoparticles. A histogram was made to relate the particle size distribution and its relationship with the array of nano-holes in the mask.

IV. Results

Nine different experiments involving both short and long pulsed beams were carried out, with multiple trials performed for each setup. Table 1 lists the specific experimental parameters for each setup. The results of these nine experiments, are described below.

TABLE I. Experimental trials and parameters

Setup Number	Pulse Width (FWHM)	Average Power	Peak Power	Energy Fluence	Mask Orientation (Alumina)
1	10 ns	0.45 W	45 MW	1.6 J/cm^2	Gold on bottom
2	10 ns	0.34 W	34 MW	1.2 J/cm^2	Gold on bottom
3	10 ns	0.23 W	23 MW	0.8 J/cm^2	Gold on bottom
4	10 ns	0.10 W	10 MW	0.35 J/cm^2	Gold on bottom
5	230 μs	0.10 W	435 W	0.35 J/cm^2	Gold on bottom
6	230 μs	0.10 W	435 W	0.35 J/cm^2	No gold coating
7	230 μs	0.23 W	10 kW	0.8 J/cm^2	No gold coating
8	10 ns	0.23 W	23 MW	0.8 J/cm^2	No gold coating
9	230 μs	0.10 W	435 W	0.35 J/cm^2	Gold on top

In experiments 1-3, the alumina membrane was completely destroyed in the irradiated area due to the high intensity of SPs. The pore structure of the alumina in this area was damaged and only fragmented pieces of alumina and gold remained in the exposed area. In experiments 4 and 5, a noteworthy result occurred. In these trials, the laser beam irradiated the alumina membrane resulting in clean ablation and subsequent deposition of gold nanoparticles on the surface of the silicon substrate. The pore structure of the alumina membrane in this case was

undamaged while the gold underneath the alumina in the exposed area was removed and deposited onto the wafer's surface. Figure 5 shows the nanoparticles embedded on silicon. Figure 6 shows the SEM image of the mask after laser irradiation. The intriguing aspect of this experiment is the low energy fluence and long pulse width of the laser beam in setup 5 that was needed for the fragmentation of the gold thin film. Various studies of nanosecond pulsed laser ablation in gas or liquid media indicate that threshold fluence required for gold thin films is approximately 5-8 J/cm^2 [3]. For the femtosecond pulsed laser ablation, threshold fluence is approximately 1.5 J/cm^2 [26]. For long pulses such as microseconds, threshold fluence is expected to be much higher. In the described work, 0.35 J/cm^2 was sufficient to ablate a significant amount of gold in the exposed area. A comparison with direct laser ablation suggests that surface plasmons substantially reduced the threshold fluence for ablation of gold. To further validate this result, setup 5 was repeated several times under the same conditions while irradiating different sections of the gold/alumina mask. Each of these new tests yielded the same result as before with the formation of gold nanoparticles on the surface of the substrate and no visible damage to the pore structure of the alumina membrane.

Under infrared wavelengths, gold has been shown to induce plasmons at the surface of a dielectric interface [27]. In this case, the alumina membrane acts as both the dielectric material and a periodic enhancer of localized surface plasmons. The 200 nm pores in the alumina membrane serve as the periodic sub-wavelength apertures in the system as discussed in the theory section. Since the gold layer is deposited via electron beam deposition, the resulting layer takes on the shape of the supporting periodic alumina layer, allowing for the resonant enhancement to occur on the semi-periodic gold layer. By inducing surface plasmons at the surface of the gold interface, microablation of the gold can occur at energy levels much lower

than that of direct laser ablation. To lend credence to this observation, we will examine the results from experimental setups 6-9. In setup 8, an alumina membrane without a gold coating was subjected to the same orientation, peak power, and pulse time as setup 3.

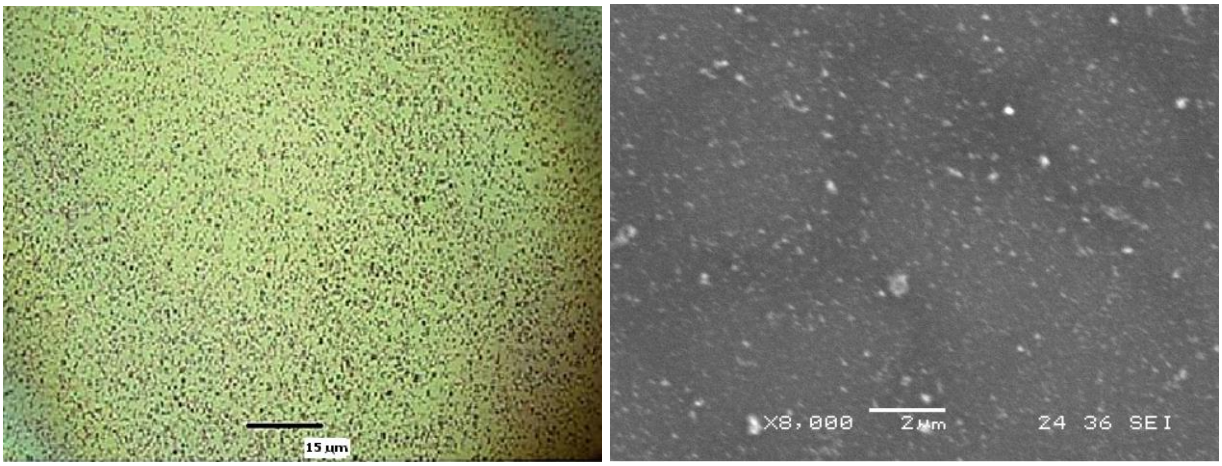

(a) Optical image **(b) SEM image**

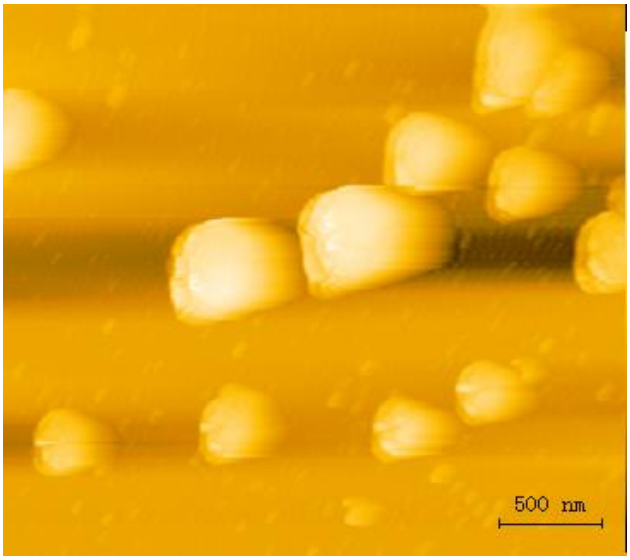

(c) AFM image

FIG. 5. Gold nanoparticles on the surface of silicon substrate (setup 5)

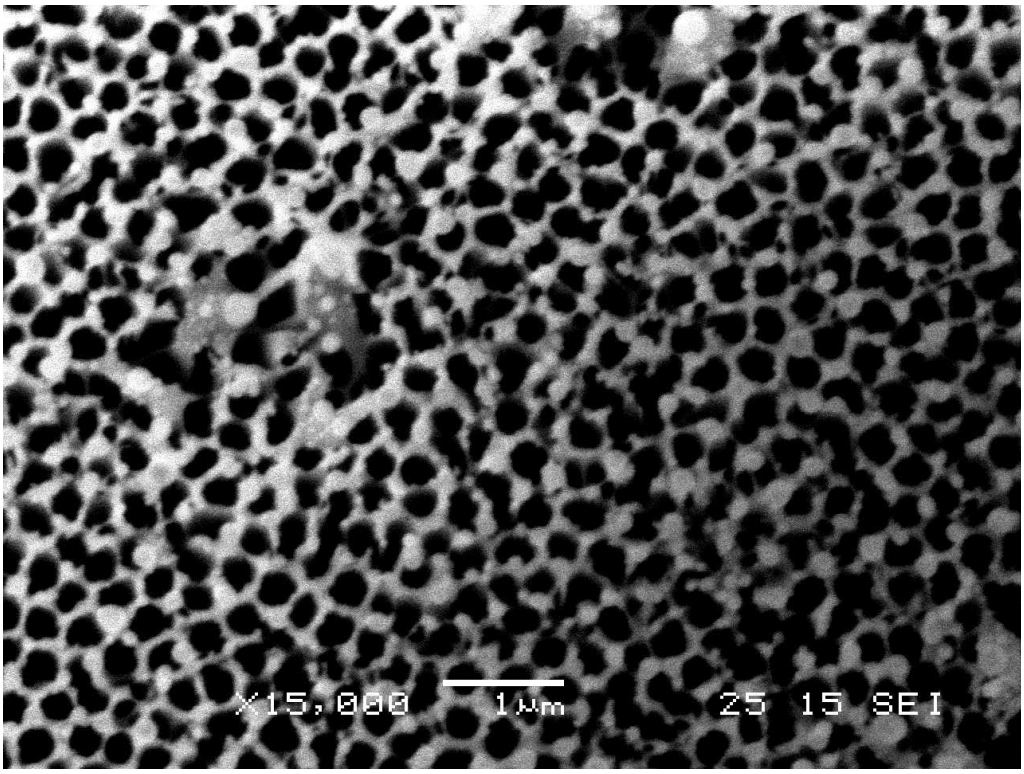

FIG. 6. SEM image of the mask after laser irradiation

In this setup, the alumina membrane pore structure was completely undamaged at the location of irradiation, suggesting that the alumina membrane was not damaged as a result of the initial energy of the laser in experiments 1-3, but as an effect of the creation of a surface plasmon wave at the interface of the gold/alumina. In setup 9, the gold-coated alumina membrane was placed in contact with the silicon substrate as before with the exception that the gold coated side was placed facing up and the non-coated side of the mask was in direct contact with the substrate. A long pulse with peak power of 0.1 W was used in a similar fashion as in setup 5. Following exposure by the Nd:YAG laser, the pore structure of the alumina membrane in setup 9 was found undamaged; however no ablation or deposition of metallic gold nanoparticles had occurred. It is apparent that the alumina membrane is important in the production of surface plasmons in our setup due to its favorable dielectric properties and periodic nature. In many cases, air can act as

the dielectric medium for inducing surface plasmons at the interface of a metal. In setup 9, the air/gold interface was unable to resonantly excite the strong surface plasmon wave that is needed to result in the ablation of gold.

Now that we have examined the mechanism behind the formation of gold particles in this experiment, we can begin to discuss the size, periodic nature, and distribution of these gold particles. Following the deposition, several optical and SEM images were taken of the gold nanoparticles on the surface of the silicon substrate. Upon analyzing these images, it is clear that the majority of the particles found on the surface have diameters in the range of 100-300 nm. Figure 7 shows a histogram of the average distribution of particle size per 15 μm square area. Results are consistent with the size of the pores in the alumina membrane and suggest that the size of the nanoparticles can very likely be easily influenced by adjusting the pore size of the alumina membrane. The controllability of the size of gold nanoparticles is a highly sought after trait due to its ever-growing applications in medicine and plasmonics based nanofocusing devices.

While the particles shown in the images presented do not appear to be highly periodic in nature, there does appear to be an even distribution of particles on the surface of the substrate. As evidenced by the images of the mask following exposure, it appears that the ablation of the gold generally occurs at the pores or near the edges of the pores in the mask and not the actual alumina. Because of this, the gold particles formed on the surface of the substrate take on the semi-periodic nature of the membrane and provide an even distribution of particles. Upon initial deposition, the gold nanoparticles in reality may have a slightly more periodic nature than what is shown in the optical and SEM images. After the experiment is performed, the surface of the

substrate could potentially be disturbed due to the nature of moving the wafer during examination and imaging.

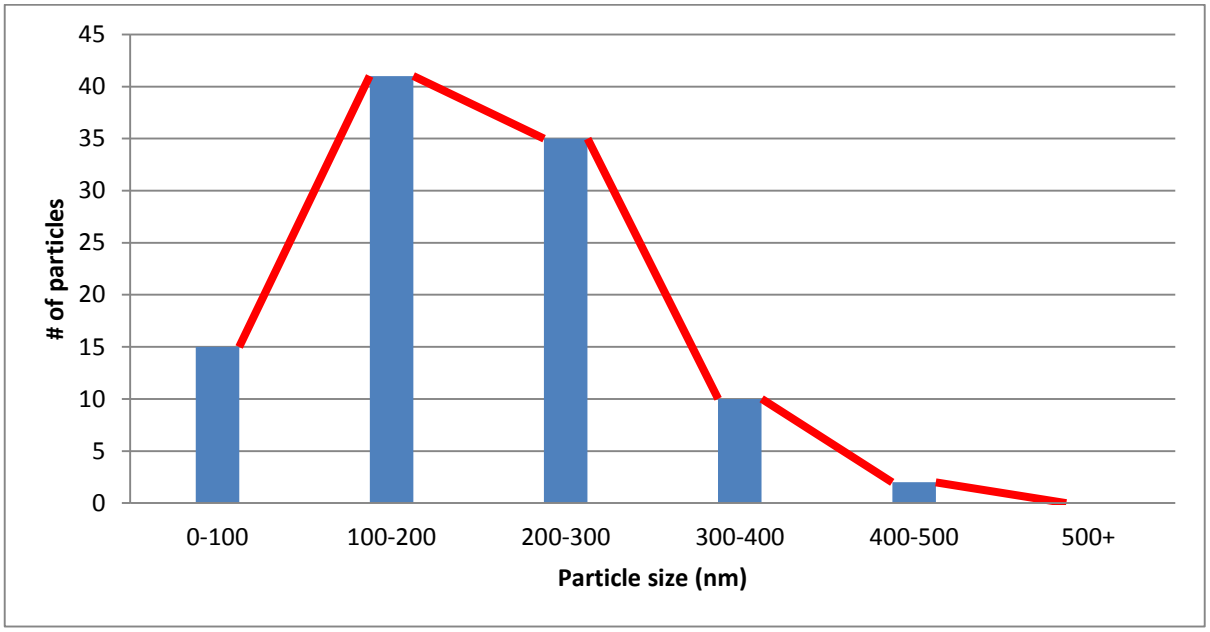

FIG. 7. Size distribution of gold nanoparticles on the silicon substrate

V. Discussion

The results of the experiment appear to show that highly energetic surface plasmons are formed during our process, resulting in the fragmentation of thin gold film to nanoscale particles. To validate this claim, we will examine whether surface plasmon resonance (SPR) conditions are met in our experiments. For 1064 nm wavelength light, the dielectric constant of alumina is a real number with a value of 10, while the dielectric constant of gold is a complex number with a value of -50+4*i* [28]. Application of equations (1) and (4) in the present study provide that the wavelength of the SP is 300 nm and periodicity for SPR condition to occur is 300 nm, 425 nm, 602 nm (1^{st}, 2^{nd}, and 3^{rd} resonance modes) respectively. In our case, the wavelengths of the

surface plasmons are much shorter than the incident light and the 2nd resonance mode of the periodic enhancement matches the average period of the mask.

The most exciting result of the study is the ability for SPs to ablate gold thin film at low energy fluence for long pulse width of incident laser light. For a gold target directly ablated by a laser, threshold fluence is given by [29]:

$$\text{Threshold (J/cm}^2\text{)} = 0.049\ (\text{pulse width in ps})^{1/2} \quad (5)$$

Application of equation (5) in direct laser ablation yields a threshold fluence of 743 J/cm^2 for 230 μs pulse and 0.5 J/cm^2 in 10 ns pulse. It may be noted that threshold fluence is also a function of wavelength which is not displayed in equation (5). The fact that SPs require only 0.35 J/cm^2 for the 230 μs incident light indicates that the mechanism of material removal in this process is different from typical thermal ablation encountered in 1064 nm laser irradiation. In a study on the 532 nm, 10 ns pulsed laser irradiation of the system air/gold film/glass under the conditions of surface plasmon resonance (SPR), a threshold fluence of 5.5 J/cm^2 was reported to produce gold nanoparticles [3]. Without SPR conditions, threshold fluence was found to be 8 J/cm^2. The mechanism accounting for material fragmentation under SPR conditions was thermal phase transition (melting and consequent micro-abalation) with a corresponding space modulation and subsequent partial nanostructure formation [3].

Results obtained in the present work did not offer any evidence for thermal damage like melting or evaporation thus eliminating thermal ablation as a possible mechanism. The non-thermal ablation mechanisms include Coulomb explosion and electrical field intensity evaporation. Typically an atom (ion) can be removed from a solid if its total energy exceeds the binding energy (i.e., the energy of vaporization per particle). In a metal like gold, Coulomb

explosion works under very high intensity and short pulse duration of the energy source because all energy losses due to electron–ion Coulomb collisions and heat conduction must be negligible. While the intensity of the laser light used during the experiment would not normally result in Coulomb explosion in gold film, the added effect of the extraordinary surface plasmon wave and adiabatic focusing allows for significantly higher effective intensities to be produced and for Coulomb explosion to occur in the gold ions. The authors believe the operating mechanism in the present study is electrical field enhancement in the vicinity of nano-holes where field-induced repulsive forces caused thin film fragmentation. The metal/dielectric mask works like an optical antenna exciting a huge electric field enhancement at the interface between alumina and gold film. Modeling the nano-hole array mask as a dipole antenna, the increase in electrical field intensity is dependent on the shape, radius and length of nano-holes in the mask. Electric field intensity enhancement can be estimated by assuming a small taper in the hole in the porous alumina membrane and using Gramotnev's model of adiabatic nanofocusing [30]. Different structures including sharp metal tips, dielectric conical tips covered in metal film, sharp V grooves and nanowedges etc. have been suggested for nanofocusing of plasmons [30]. Here we assume that the taper begins at one side of the pore in alumina and ends on the opposite opening at an infinitely sharp point. Due to the nature of the sputtering process, the top of the walls of the alumina pores will likely contain a thin layer of gold film, allowing us to approximate our system as a sharp V dielectric groove covered in metal film. From the pore diameter and thickness of alumina membrane, we approximate the taper angle $\beta \approx 0.0033$. According to Gramotnev's model of adiabatic nanofocusing [30], electrical field enhancement would occur if

$$\beta < \beta_c = -2\,{\varepsilon_d}/{\varepsilon_m}' \quad (6)$$

where $\varepsilon_d = 10$, $\varepsilon_m{}' = -50$ and thus $\beta_c = 0.4$. Since $< \beta_c$, significant enhancement of the electric field can occur *assuming no plasmon energy dissipation in the metal*. Although the electric field will theoretically be infinite at the location of "zero radius" tip, this would not be the case in practice. At distances of $10^{-2}\mu$m from the tip, the electric field enhancement is estimated to be around 100-150 times the normal value [30]. Thus, the high field enhancement factor induces dipole moments in gold and thereby pulling the atoms and grains out of gold.

The surface plasmon method described in this work is simpler, quicker, energy efficient, contamination-free, and environmentally safer than existing physical and chemical methods. The technique can be readily extended to all types of materials. A well-known physical technique for gold is pulsed laser ablation (PLA) in vacuum or gaseous environment and is widely used to produce nanoparticles collected in the form of nanopowder [16]. Although PLA does not require high temperature or a chemical reaction, it is limited by the need for a high vacuum, high energy fluence, and long pumping time. In addition, the broader distribution of nanoparticles is a problem. An improved PLA for gold nanoparticles is performed by immersing the gold target in a liquid medium leading to functionalized gold nanoparticles with a ligand of choice in a colloidal solution. For example, 532 nm, 7 ns Nd:YAG laser ablation of gold target at 79 J/cm^2 in distilled water produced colloidal gold nanoparticles [9]. The main difference between ablation in gas and in liquid is that liquid produces a stronger confinement of the expanding plasma plume generating higher temperatures and pressures and causing the vaporization of the liquid/chemical reactions and much broader distribution of nanoparticles [16-19]. It has been shown that laser ablation in liquid produces surface-charged nanoparticles with a shell of dipole molecules (e.g., water) formed around them, preventing agglomeration. Stable gold nanoparticles were synthesized by laser ablating gold foil placed inside ionic liquids without the addition of

any external chemical reagent [18]. Commercialization of laser ablation in liquids was launched by *Particular GmbH* for the production of gold nanoparticles in a variety of biophotonic applications.

The other well defined process group used in the formation of gold nanoparticles is through chemical means, which is based on the synthesis of compounds to extract gold particles from a chemical system. Simple chemical reduction methods can produce 5–100 nm nanoparticles but the surface of these nanoparticles are often contaminated with reaction by-products such as anions and reducing agents, which can interfere with subsequent stabilization and functionalization steps [20]. Nakamoto [10] produced 11 to 76 nm gold particles by the controlled thermolysis of ammonium gold (I) thiolate. Arshi [11] used a hybrid method involving chemical mixing and microwave heating to produce average particle size of 4 nm.

While these are just a few example techniques used to manufacture gold nanoparticles, the applications of these techniques are just as diverse and far-reaching. Cherukuri and Curley [12] discussed the applications of gold nanoparticles in the treatment of malignant cells. Gold nanoparticles conjugated with cetuximab are shown to be quickly internalized by pancreatic and colorectal cancer cells in the human body. Following internalization, a non-invasive/non-ionizing radiofrequency field is focused in the affected area of the body. This exposure resulted in the heating of the gold nanoparticles and surrounding malignant cells. The treated cells showed a cytotoxicity rate of almost 100%. In the microelectronics industry, gold nanoparticles bring exciting new possibilities to photovoltaic cells and conventional lithography. Colloidal silver and gold nanoparticles are used to trap light on the surface of silicon photovoltaic cells [13]. By taking advantage of the plasmonic tendencies of gold nanoparticles, it has been shown that an enhancement of the photovoltaic conversion efficiency can occur. When compared to

similar silicon solar cells without gold nanoparticles, the new solar cells showed a significant increase in the external quantum efficiency under visible and near-infrared light due to the effect of plasmonic light scattering. In lithography, the use of gold nanoparticles can be used to help effectively overcome the diffraction limit of light. Gold triangular nanoprisms patterened in a hexagonal lattice have been studied to observe their super focusing properties [14].

VI. Conclusion

The work presented in this paper attests to the power of surface plasmons for the ablation of gold. The excitation of surface plasmon resonance described in this technique is a low energy alternative to the traditional pulsed laser ablation for the formation of structured nanoparticles on the surface of a substrate. The plasmonic system takes advantage of a novel use of porous alumina membrane as an effective dielectric with periodic sub-wavelength aperture enhancement of localized surface plasmons at the interface of a gold film. There is an orderly distribution of particles on the substrate with a close match between the particle size and the hole size in the mask. The results provide a strong basis for further development and applications related to laser-assisted surface plasmon excitation. Unlike other chemical techniques used to create metallic nanoparticles, the advancement of this process will allow for the deposition of particles over a broad area and allow for the particles to be transferred to any substrate in a semi-periodic fashion. The proposed technique is advantageous over other laser assisted techniques in that the process requires a lower energy density and results in a more highly ordered array of particles. The applications of the proposed technique are far-reaching and could potentially impact the advancement of microelectronic and medicinal research.

Acknowledgements

This material is based upon work supported by the National Science Foundation under Grant No. CMMI-1237275. The lead author gratefully acknowledges the financial support.

References

1. P. Molian, Z. Lin, Q. Zou. Nano-holes in silicon wafers using laser-induced surface plasmon polaritons. J Nanosci Nanotechno. **2008**, 8, 2163-2166.

2. E. Simsek, S. Akturk. Plasmonic enhancement during femtosecond laser drilling of sub-wavelength holes in metals. Plasmonics. **2011**, 6, 767-772.

3. L. Fedorenko, S. Mamykin, O. Lytvyn. Nanostructuring of continuous gold film by laser radiation under surface plasmon polariton resonance conditions. Plasmonics. **2011**, 6, 363-371.

4. N. Nikolay, Semra, A. Petar. Nanosecond laser heating of gold nanoparticles. Application in photothermal cancer cell therapy. C.R. Acad. Bulgare Sci. **2010**, 63, 767-774.

5. L. Chia-Ching, L. Mei-Yi, C. Wen-Yu. Plasmonic metallic nanostructures by direct nanoimprinting of gold nanoparticles. Opt Express. **2011**, 19, 4768-4776.

6. D. Vivek, M. Subas, L. Wonjoo. Enhanced conversion efficiency in dye-sensitized solar cells based on ZnO bifunctional nanoflowers loaded with gold nanoparticles. Appl Phys Lett. **2008**, 93, 243108.

7. J. Lin, W.L. Zhou, C.J. O'Connor. Formation of Ordered Arrays of Gold Nanoparticles from CTAB Reverse Micelles. Mater Lett. **2001**, 49, 282-286.

8. A.T. Izgaliev, A.V. Simakin, G.A. Shafeev. Formation of the alloy of Au and Ag nanoparticles upon laser irradiation of the mixture of their colloidal solutions Quantum Electron+. **2004**, 34, 47-50.

9. A.K. Singh, A.K. Rai, D. Bicanic. Controlled synthesis and optical properties of pure gold nanoparticles. Instrum Sci Technol. **2009**, 37, 50-60.

10. M. Nakamoto, Y. Kashiwagi, M. Yamamoto. Synthesis and size regulation of gold nanoparticles by controlled thermolysis of ammonium gold(I) thiolate in the absence or presence of amines. Inorg chim acta. **2005**, 358, 4229-4236.

11. N. Arshi, F. Ahmed, S. Kumar. Microwave assisted synthesis of gold nanoparticles and their antibacterial activity against Escherichia coli (E-coli). Curr Appl Phys. **2011**, 11, S360-S363.

12. P. Cherukuri, S. Curley. Use of nanoparticles for targeted, noninvasive thermal destruction of malignant cells. Cancer Nanotechnol: methods and protoc. **2010**, 624, 359-373.

13. S.K. Jana, A. Le Donne, S. Binetti. Enhancement of silicon solar cell performances due to light trapping by colloidal metal nanoparticles. J Phys Chem Solids. **2012**, 73, 143-147.

14. M. Giloan, S. Astilean. Visible frequency range negative index metamaterial of hexagonal arrays of gold triangular nanoprisms. Opt Commun. **2012**, 285, 1533-1541.

15. P.M. Boltovets, S.A. Kravchenko, B.A. Snopok. Building interfacial nanostructures by size-controlled chemical etching. Plasmonics. **2010**, 5, 395-403.

16. N. Semaltianos. Nanoparticles by laser ablation. CRC CR Rev Sol State. **2010**, 35, 105-124.

17. F. Mafuné, J. Kohno, Y. Takeda, T. Kondow. Formation of gold nanoparticles by laser ablation in aqueous solution of surfactant. J Phys Chem B. **2001**, 105, 5114-5120.

18. H. Wender**,** M.L. Andreazza**,** R.R. Correia**.** Synthesis of gold nanoparticles by laser ablation of an Au foil inside and outside ionic liquids. Nanoscale. **2011**, 3, 1240-1245.

19. D. Riabinina, M. Chaker, J. Margot. Dependence of gold nanoparticle production on pulse duration by laser ablation in liquid media. Nanotechnology. **2012**, 23, 135603.

20. J.P. Sylvestre, A.V. Kabashin, E. Sacher. Femtosecond laser ablation of gold in water: influence of the laser-produced plasma on the nanoparticle size distribution. Appl Phys A. **2005**, 80, 753-758.

21. S.A. Maier. Plasmonics - a route to nanoscale optical devices. Adv Mater. **2001**, 13, 1501+.

22. H. Raether. *Surface Plasmons on Smooth and Rough Surfaces and on Gratings*. Springer Tracts in Modern Physics, 1988; 11.

23. R. He, X. Zhou, Y. Fu. Near-field optical experimental investigation of gold nanohole array. Plasmonics. **2011**, 6, 171-176.

24. Y.K. Zhang, X.C. Dong. Nanolithography method by using localized surface plasmon mask generated with polydimethylsiloxane soft mold on thin metal film. Opt Lett. **2010**, 35, 2143-2145.

25. A. Degiron, T.W. Ebbesen. The role of localized surface plasmon modes in the enhanced transmission of periodic subwavelength apertures. J Opt A-Pure Appl Op. **2005**, 7, S90-S96.

26. J. Krueger, D. Daniela. Femtosecond laser-induced damage of gold films. Appl Surf Sci. **2007**, 253, 7815-7819.

27. W. Zhong, Y. Wang, R. He. Investigation of plasmonics resonance infrared bowtie metal antenna. Appl Phys B-Lasers O. **2011**, 105, 231-237.

28. H. Xie, F.M. Kong, K. Li. The electric field enhancement and resonance in optical antenna composed of Au nanoparticles. J of Electromagn Waves and Appl. **2009**, 23, 535-548.

29. E.G. Gamaly, A.V. Rode, V.T. Tikhonchuk. Ablation of solids by femtosecond lasers: ablation mechanism and ablation thresholds for metals and dielectrics. Phys Plasmas. **2002**, 9, 949-957.

30. D.K. Gramotnev, D. Pile, M. Vogel. Local electric field enhancement during nanofocusing of plasmons by a tapered gap. Phys Rev B. **2007**, 75, 035431.

CHAPTER 3. PLASMONIC NANOLITHOGRAPHY AND NANOTEXTURING OF PHOTORESIST USING A SIMPLE MASK

A paper to be submitted to Material Letters

Quincy Garner and Pal Molian

In this paper, the authors present a low-cost lithography technique utilizing surface plasmons. The photomask is a porous alumina membrane coated with a thin layer of aluminum. A coherent, 337 nm UV laser source is used to expose the photomask and excite surface plasmons along the metal layer. The surface plasmons allow for features well below the wavelength of the incident light to be produced in photoresist. Along with this technique, an alternative technique has been developed using a 405 nm UV lamp to produce a labyrinth texturing effect and periodic micro-features.

Keywords: surface plasmon polaritons; photolithography; porous alumina membrane

1. Introduction

Plasmonics is a rapidly growing technology for photonics, sensors, microscopy, data storage, and lithography. For example, plasmonic photolithography based upon the theory of surface plasmon polaritons (SPPs) is widely perceived as the next generation lithography for validating Moore's law. Surface plasmon polaritons (SPPs) are generated at the interface between metal and dielectric when light impinges on nanoscale perforated metallic thin film. SPPs exhibit much smaller wavelength compared to that of the incident light following the unique dispersion relation [1]:

$$k_{sp} = \left(\frac{2\pi}{\lambda_0}\right)\sqrt{\frac{\varepsilon_d \varepsilon_m}{\varepsilon_d + \varepsilon_m}} \quad (1)$$

where λ_0 is the incident light wavelength in vacuum, ε_d is the permittivity of the dielectric material, and ε_m is the permittivity of the metal material. Surface plasmons exist in two basic forms: propagating (PSP) and localized (LSP). Along the metal-dielectric interface, the PSP propagates as an evanescent electromagnetic wave resulting from the collective oscillations of the free electrons in the conduction band in the metal surface. In most cases, SPPs are not easily excited due to the momentum difference between the incident light waves and surface plasmon waves. To compensate for this, periodic arrays of holes in the thin films are necessary to account for the momentum mismatch and excite the SPPs [2, 3]. LSPs do not propagate in the horizontal plane, but rather exist as localized electromagnetic fields near the surface of isolated nanoparticles or nanohole arrays and assist in the transmission of light through sub-wavelength apertures. For periodic sub-wavelength apertures, the total transmission enhancement is explained as the integrated effect of LSPs and PSPs[4]:

$$\lambda_{\max}(i,j) = P(i^2 + j^2)^{-\frac{1}{2}}\sqrt{\frac{\varepsilon_1 \varepsilon_2}{\varepsilon_1 + \varepsilon_2}} \quad (2)$$

where $\lambda_{max}(i,j)$ is the wavelength of peak light transmission, P is the lattice constant, i and j are the scattering orders from the array, ε_1 and ε_2 are respectively the dielectric constants of the metal and the dielectric material. Each peak of the light transmission is labeled by a set of integers (i, j).

Using the dispersion and transmission of light phenomena described above, many nanolithography systems have been developed that overcome the diffraction limit of the incident light [5-12]. However, the bottlenecks of these plasmonic systems are weak plasmon exposure in photoresists due to the use of UV lamps with low intensity; costly, shape-limiting and time-consuming fabrication of the plasmonic lenses based on grating, Fresnel pattern and slab of silver; near field processing with difficulties in positioning control systems; and serial nanofabrication schemes. Most notable of these issues is the inherently low throughput of these systems due to the methods by which the photomask is fabricated. In most cases, the patterns on a mask are generated using focused ion beam (FIB) or electron beam writer technology. These writing systems can limit the throughput and complexity of a lithography mask due to their relatively slow writing speeds. Along with these limitations, FIB and e-beam writer systems can be prohibitively expensive, which in turn drives up the cost of each mask produced. Alternative nanofabrication techniques such as nanoimprint lithography and plasma dry etching have been used to successfully pattern nanoscale features at relatively high throughput, but are limited by repeatability issues, cost, and damage to the mask. Techniques using silica microbeads to focus light on the levels of λ⁄15 have been developed, but add complexity to the system by introducing extra steps for assembling and removing unwanted particles [13,14], which in turn lower the total throughput of the system. Thus, there exists a need to develop a method for producing low-cost masks capable of producing sub-diffraction limited features at a high throughput using simple

UV light sources. In this paper, we focus on designing an easy-to-fabricate, inexpensive and durable photomask and investigating its effects in nanolithography.

2. Material and Methods

We devised a simple photomask of aluminum/alumina interface acting as the metal/dielectric boundary to address the two main issues of high cost and low throughput in the plasmonic masks. Alumina having very high dielectric constant is robust and durable. Aluminum is chosen for its ability to excite surface plasmons in the UV range [1]. Pores in the dielectric alumina layer act as the periodic hole array capable of resonantly generating SPPs along the aluminum boundary. To fabricate the plasmonic photomask for our experiments, a pre-made Whatman Anopore aluminum oxide membrane (PAM) with pore diameters of approximately 0.2 μm was coated with a 50 nm layer of aluminum via electron beam deposition (Figure 1). The pores in the membrane are semi-periodic in nature with center to center period of 0.2 μm.

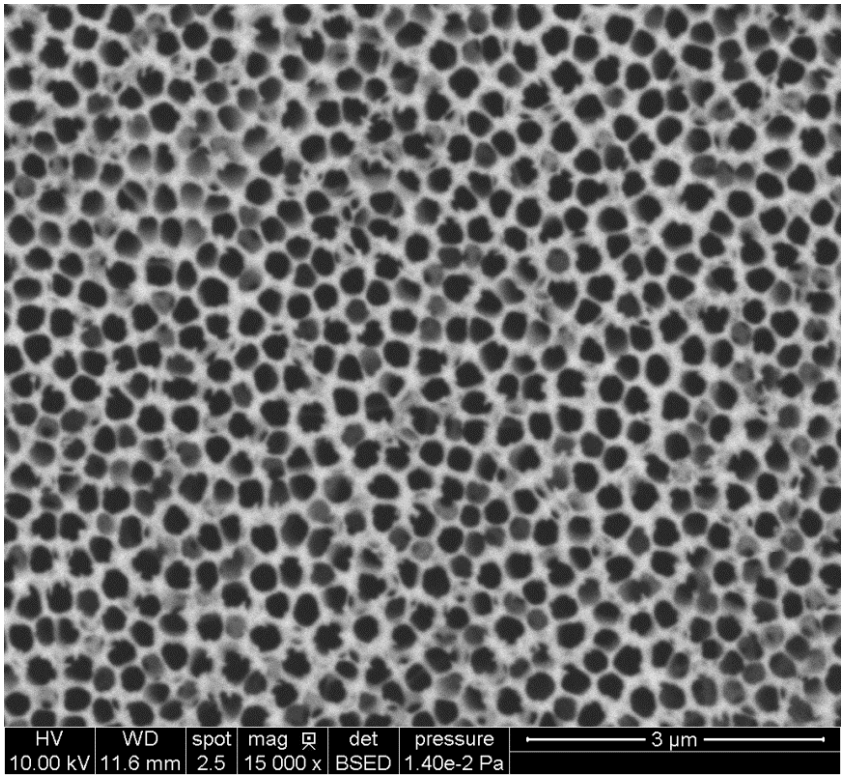

FIG. 1. Porous alumina membrane coated with a 50 nm layer of aluminum (plasmonic photomask)

3. Results

Two independent experiments were conducted using two different low-cost UV light sources. In the first experiment, the mask is placed in direct contact with a silicon wafer spun coated with SU-8 photoresist. The aluminum side of the mask is placed facing up and away from the wafer. A p-polarized, VSL 337.1 nm nitrogen laser was incident perpendicularly across the surface of the photomask and exposed for 20 seconds. The exposure resulted in a total dosage of approximately 400 mJ/cm^2, over a total area of 0.35 cm^2. Following exposure and development, the wafer was examined to see if the alumina pore pattern had transferred to the photoresist. Using an atomic force microscope (AFM), several bands of exposed photoresist

patterns were discovered. In these exposed areas, many features in the range of 200-300 nm were found in a similar pattern to that of the pores in the alumina membrane (Figure 2); this technique was able to produce features as small as 100 nm due to the variation in pore diameters of the PAM (Figure 3). In a conventional photolithography system, the minimum linewidth of a pattern that can be successfully replicated is given by approximately $\lambda/2$. In our system, linewidths of $\lambda/3$ were fabricated, suggesting an enhanced transmission likely occurred due to the creation of localized surface plasmons in some locations across the plasmonic mask. Features that appear to be slightly larger than the pore diameter can be attributed to the enhanced transmission of light due to the formation of localized surface plasmons as well as the slight air gap between the mask and photoresist layer. The penetration depths of the patterns on the photoresist appear to be quite shallow due to the near-field property of the surface plasmon mode. This may cause issues when transferring the pattern to other materials, but can be easily remedied by using a different resist or thinner resist layer.

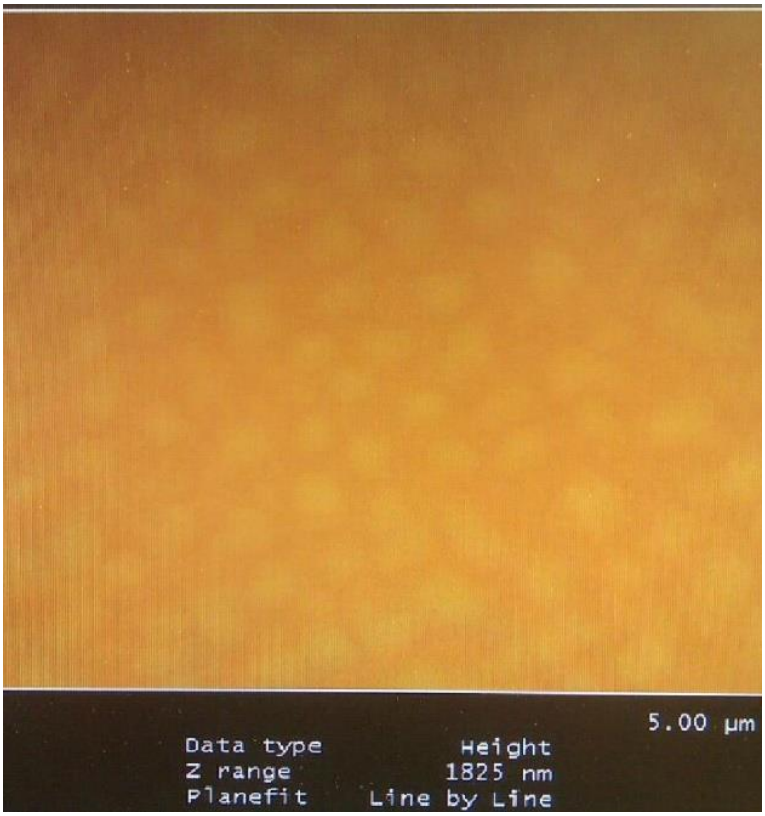

FIG. 2. AFM image of exposed SU-8 photoresist with plasmonic photomask pattern

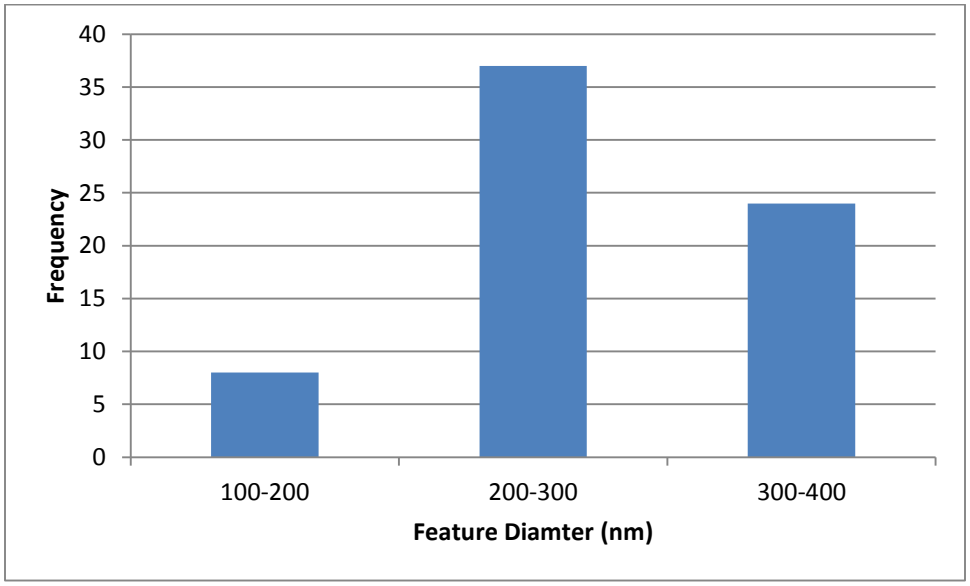

FIG. 3. Histogram of average frequency of individual feature diameter in 5 µm x 5 µm exposed area

In the second experiment, a 405 nm peak filtered Mercury lamp was used instead of the 337 nm laser. The aluminum covered membrane was again used as the photomask with the aluminum side facing opposite to the silicon wafer as before. AZ-5214E photoresist was used for this experiment instead of SU-8. The system was exposed to a total dosage of 150 mJ/cm^2 across the photomask. Following exposure and development, the wafer was examined via an optical microscope and scanning electron microscope (SEM). In the two SEM images (Figure 4), it is seen that instead of completely transferring the PAM pattern onto the photoresist, a labyrinth texturing pattern was instead created. The formation of this texturing pattern can be attributed to a combination of the diffraction of light through the pores in the alumina membrane and the edge effect at the pore boundary. Due to a slight roughness at the pore boundary between the aluminum/alumina interface, the incident light that is unable to focus through the pore becomes scattered, resulting in the labyrinth pattern shown. At many areas throughout the alumina membrane, the pores are not highly periodic and thus localized surface plasmons cannot easily be generated. The SPPs generated in this case are alone not enough to overcome the diffraction limit of the 200 nm diameter pores. In the two optical images shown (Figure 5), it appears that the PAM pattern was able to transfer to the photoresist in a limited extent. The features shown in the photoresist layer appear to represent the PAM pattern with the exception that the features are significantly larger and spread further apart than the pattern of the pores in the PAM. The pattern is attributed to the presence of localized surface plasmons created by the semi-periodic nature of the aluminum on the alumina membrane. Since the membrane pattern is not homogeneously periodic in all locations, localized surface plasmons will only be generated in certain spots along the surface of the aluminum. These spots resulted in enhanced transmission

and the transfer of the pore pattern. Larger feature sizes are again attributed to the formation of LSPs and the slight air gap between the photomask and wafer. To further minimize the feature sizes created in this process, the mask dimensions, exposure dose and development technique will likely need to be optimized. In the areas where localized surface plasmons cannot be resonantly generated, the textured labyrinth pattern seems to appear in the same manner as the SEM images as shown before.

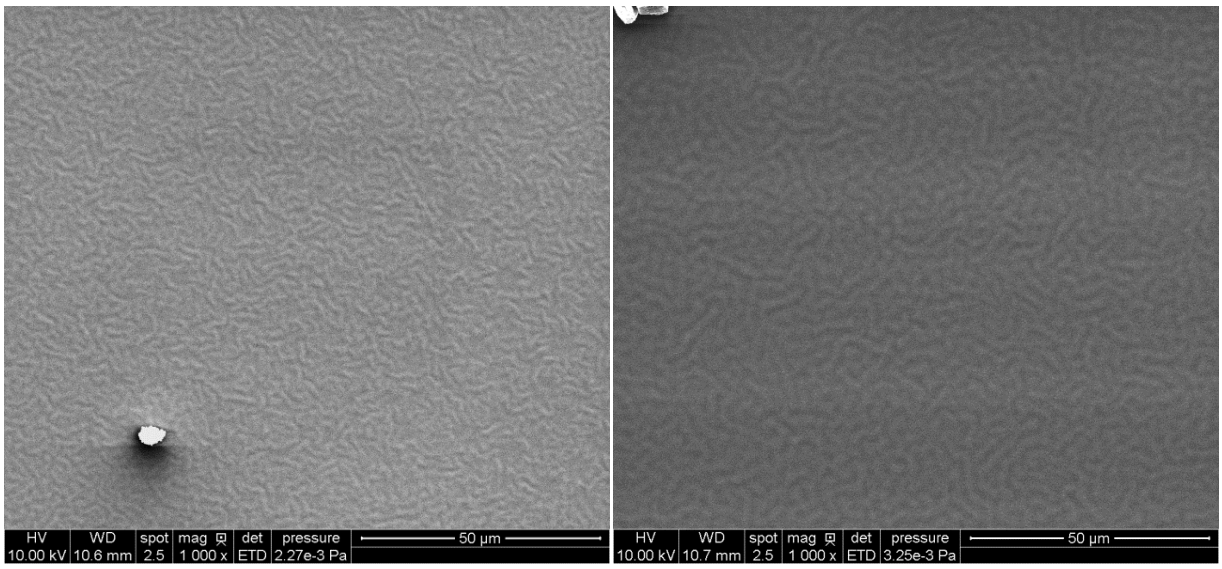

FIG. 4. SEM images of exposed AZ 5214 E photoresist with labyrinth texturing pattern

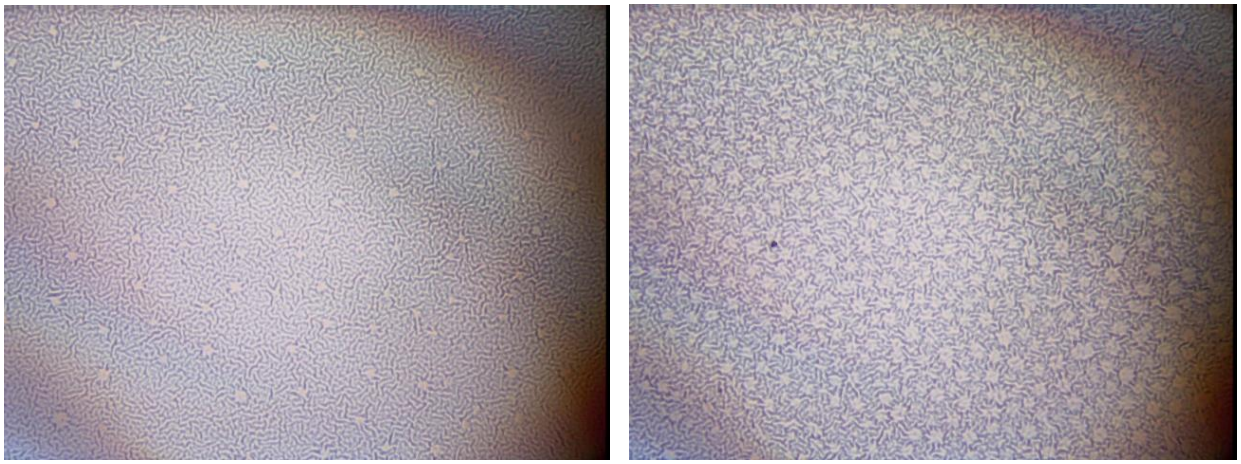

FIG. 5. Optical images of exposed AZ 5214 E photoresist with periodic micro features (1000x)

To determine whether the metal-dielectric interface and the formation of surface plasmons were the main contributing factors in our process, a porous alumina membrane with no aluminum coating was subjected to the same photolithography processes as in the previous experiments. Following exposure and development, the wafer was once again examined using SEM and optical microscopy. After close examination, it was revealed that the porous alumina pattern was not transferred to the photoresist, suggesting the metal-dielectric interface played a crucial role in the lithography process.

4. Conclusion

The simple plasmonic photomask and subsequent fabrication techniques demonstrated in this letter provide a unique solution to the issues hampering the use of plasmonics in photolithography. Through the use of a pre-fabricated porous alumina membrane coated with a thin layer of aluminum, features on the scale of $\lambda/3$ were demonstrated with relatively high throughput using a simple 337 nm UV laser. A surface labyrinth texturing effect and periodic

micro features were realized using the same plasmonic photomask with a 405 nm peak UV lamp. Through process optimization and improved consistency in the alumina dielectric layer, the techniques shown in this letter have the potential to provide a low cost, simple, high throughput alternative to the semiconductor industry.

This material is based upon work supported by the National Science Foundation under Grant No. CMMI-1237275. The lead author gratefully acknowledges the financial support.

References

1. H. Raether. Surface Plasmons on Smooth and Rough Surfaces and on Gratings. Berlin:Springer; 1988.

2. Y.K. Zhang, X.C. Dong, J.L. Du, X.Z. Wei, L.F. Shi, Q.L. Deng, C.L. Du. Nanolithography method by using localized surface plasmon mask generated with polydimethylsiloxane soft mold on thin metal film. Opt Lett 2010; 35:2143-2145.

3. A. Degiron, T.W. Ebbesen. The role of localized surface plasmon modes in the enhanced transmission of periodic subwavelength apertures. J Opt A-Pure Appl Op 2005; **7**:S90-S96.

4. A. Krishnan, T. Thio, T.J. Kima. Evanescently coupled resonance in surface plasmon enhanced transmission. Opt Commun 2001; 200:1-7.

5. W. Srituravanich, N. Fang, C. Sun, Q. Luo, X. Zhang. Plasmonic nanolithography. Nano Lett 2004; 4:1085-1088.

6. S. Seo, H.C. Kim, H. Ko, M. Cheng. Subwavelength proximity nanolithography using a plasmonic lens. J Vac Sci Technol B 2007; 25:2271-2276.

7. H.W. Gao, J.K. Hyun, M.H. Lee, J.C. Yang, L.J. Lauhon, T.W. Odom. Broadband plasmonic microlenses based on patches of nanoholes. Nano Lett 2010; 10:4111-4116.

8. Z.W. Liu, J.M. Steele, W. Srituravanich, Y. Pikus, C. Sun, X. Zhang. Focusing surface plasmons with a plasmonic lens. Nano Lett 2005; 5:1726-1729.

9. J.M. Steele, Z.W. Liu, Y. Wang, X. Zhang. Resonant and non-resonant generation and focusing of surface plasmons with circular gratings. Opt Express 2006; 14:5664-5670.

10. Y.Q. Fu, Y. Liu, X.L. Zhou, Z.W. Xu, F.Z. Fang. Experimental investigation of superfocusing of plasmonic lens with chirped circular nanoslits. Opt Express 2010; 18: 3438-3443.

11. L. Wang, S.M. Uppuluri, E.X. Jin, X.F. Xu. Nanolithography using high transmission nanoscale bowtie apertures. Nano Lett 2006; 6:361-364.

12. K. Ueno, S. Takabatake, K. Onishi, H. Itoh, Y. Nishijima, H. Misawa. Homogeneous nano-patterning using plasmon-assisted photolithography. Appl Phys Lett 2011; 99:011107.

13. Y. Lu, S.Theppakuttai, S.C. Chen. Marangoni effect in nanosphere-enhanced laser nanopatterning of silicon. Appl Phys Lett 2003; 82:4143-4145.

14. A. Battula, S. Theppakuttai, S.C. Chen. Direct, parallel nanopatterning of silicon carbide by laser nanosphere lithography. J Microlith Microfab 2006; 5:011009.

CHAPTER 4. GENERAL CONCLUSIONS

4.1 Summary

From the results of the previous two chapters, it is apparent that the use of plasmonics for micro/nano manufacturing purposes has the ability to revolutionize the semiconductor industry. In chapter 2, a method for generating a wide array of semi-periodic gold nanoparticles via an optical plasmonic antenna was discussed. In this technique, a gold/alumina nano-hole optical antenna can be irradiated using a 1064 nm Nd:YAG laser system, depositing semi-periodic gold nanoparticles onto the surface of any flat substrate. The discussed method shows great potential as a low cost, simple, low energy, and environmentally friendly alternative to other nanoparticle formation techniques in literature. In chapter 4, a low cost plasmonic nanolithography photomask capable of producing features on the order of $\lambda/3$ is discussed. This technique utilizes the dielectric properties of aluminum oxide with the ability of aluminum to produce surface plasmon effects at UV wavelengths. Periodic nanohole arrays in the alumina allow for localized surface plasmons to develop on the surface of the aluminum film and expose features in the photoresist that would not be reproducible without a plasmonic effect. This method provides a great low cost alternative to conventional photolithography and other more complex plasmonic nanolithography setups.

4.2 Recommendations

The main focus of this study was to investigate the potential applications of plasmonics in micro/nanomanufacturing. While the work presented in the previous chapters has shown a few possible uses of plasmonics in manufacturing, more work can be done to build upon the results of this paper. One of the most impactful advances that could benefit the discussed techniques

would be the development of a more consistent and highly periodic alumina membrane. The membranes used in the discussed research were developed for purposes unrelated to their actual application. An alumina membrane with consistent periodic features would allow for stronger coupling of light with the deposited metal film and a more widespread localized surface plasmon resonance to occur. With a stronger resonance effect, we could potentially see ablation of gold nanoparticles at even lower energy fluence levels than what was observed using the gold/alumina optical antenna. In the plasmonic nanolithography technique, a stronger localized surface plasmon effect has the potential to produce features smaller than the $\lambda/3$ features previously shown if minor adjustments are made to the pore sizes of the mask.

The plasmonic nanohole optical antenna technique has the versatility to be used with various metals exhibiting a plasmonic response under certain wavelengths. UV and visible wavelength light sources could be used to develop a technique for depositing silver and aluminum nanoparticles in a similar manner to the gold nanoparticle technique.